Title

Reduced Inotropic Effect of Nifekalant in Failing Hearts in Rats

Hideaki Endo, Masahito Miura, Masanori Hirose, Jun Takahashi, Makoto Nakano,

Yuji Wakayama, Yoshinao Sugai, Yutaka Kagaya, Jun Watanabe, Kunio Shirato,

Hiroaki Shimokawa

Department of Cardiovascular Medicine,

Tohoku University Graduate School of Medicine, Sendai, Japan

(H.E., M.M., M.H., J.T., M.N., Y.W., Y.S., Y.K., J.W., K.S., H.S.).

Running title

No Positive Inotropic Effect of Nifekalant in Heart Failure

Address for correspondence and reprints:

Masahito Miura M.D., Ph.D.

Department of Cardiovascular Medicine

Tohoku University Graduate School of Medicine

1-1 Seiryo-machi, Aoba-ku, Sendai 980-8574, Japan

Tel: 81-22-717-7153, Fax: 81-22-717-7156

EM: mmiura@cardio.med.tohoku.ac.jp

Total text pages 33 with 5 figures and 2 tables

Abstract 246 words

Introduction 368 words

Discussion 1107 words

List of nonstandard Abbreviations: MCT, monocrotaline; SR, sarcoplasmic reticulum; RCC, rapid cooling contracture; SERCA2, sarcoplasmic reticulum Ca^{2+} ATPase type2; PLB, phospholamban; NCX, sodium-calcium exchanger; GAPDH, glyceraldehyde-3-phosphate dehydrogenase; CPA, cyclopiazonic acid.

Section: Cardiovascular

Abstract

Class III anti-arrhythmic agents have been widely used to suppress ventricular tachyarrhythmias in patients with heart failure as they have been shown to have positive inotropic effects as well. However, it remains to be examined whether those agents also exert positive inotropic effects in failing hearts. We addressed this important issue in a rat model of heart failure. We used nifekalant as a representative class III anti-arrhythmic agent. Four weeks after a subcutaneous injection of 60 mg/kg monocrotaline (MCT-rats) or vehicle (Ctr-rats), we obtained trabeculae from right ventricles and measured the developed force and intracellular Ca^{2+} ($[Ca^{2+}]_i$) by the fura-2 microinjection method. The sarcoplasmic reticulum (SR) Ca^{2+} content was assessed by the rapid-cooling contracture (RCC) technique. MCT-rats exhibited right ventricular hypertrophy induced by pressure overload. The protein expression of SR Ca^{2+} ATPase type2 (SERCA2) and the SERCA2/phospholamban ratio in MCT-rats was lower with a slower decline of Ca^{2+} transients and a reduced amplitude of RCCs. Nifekalant concentration-dependently increased the force, peak $[Ca^{2+}]_i$, and the amplitude of RCCs in Ctr-rats, but not in MCT-rats with identical prolongation of the action potential. Under the SR inhibited with cyclopiazonic acid and ryanodine, nifekalant increased the force in Ctr-rats but not in MCT-rats. These results indicate that the positive inotropic effects of nifekalant is reduced in failing hearts, probably due to the depressed SR Ca^{2+} uptake and reduced reserve of the trans-sarcolemmal Ca^{2+} transport, warranting a caution in the anti-arrhythmic therapy with a class III anti-arrhythmic agent in heart failure.

Introduction

Ventricular tachyarrhythmias often occur in patients with reduced ventricular function (Krishnan et al., 2002). Anti-arrhythmic agents may aggravate heart failure symptoms due to the potential negative inotropic effects and thereby cause cardiac decompensation in patients with heart failure. Thus, class III anti-arrhythmic agents have been widely used to suppress ventricular tachyarrhythmias in patients with heart failure as they have been shown to have positive inotropism as well (Peralta et al., 2000). However, it remains to be examined whether those agents also exert positive inotropic effects in failing hearts.

Nifekalant is a representative class III anti-arrhythmic agent with a pyrimidinedione structure (Nakaya et al., 1993). It blocks the rapid-delayed rectifier current (I_{kr}) at therapeutic concentrations between 1 and 10 μM (Shiga et al., 2001), and several other channels at concentrations above 10 μM (Mori et al., 1995), thus exerting a clinically potent suppressive action against ventricular tachyarrhythmias. The K^+ channels blocking effects of nifekalant can prolong the duration of an action potential (Sen et al., 1998) and consequently increase the muscle contraction depending on the concentration in intact rat cardiac muscle (Hirose et al., 2005).

Many animal models are available to examine the alterations in molecular and cellular responses in heart failure. Among animal models of heart failure, a rat model of monocrotaline (MCT)-induced pulmonary hypertension and right-sided heart failure is unique, as the enhanced mechanical load on the right ventricles alters the ß-adrenoceptor-G-protein(s)-adenylyl cyclase system (Seyfarth et al., 2000), the protein expression involved in the maintenance of Ca^{2+} homeostasis (Kögler et al., 2003), and the spatial distribution of gap junctions (Uzzaman et al., 2000). These

alterations are also observed in left ventricular failing models (Hasenfuss and

Pieske, 2002; Näbauer and Kääb, 1998), suggesting that the properties of the right

ventricle from monocrotaline-treated rats are similar to those of left ventricular failing

hearts. This model also has an advantage to study the alteration in electrical

properties of myocytes as it is easy to obtain multicellular cardiac muscle (e.g.

trabeculae) from the right ventricle (ter Keurs et al., 1980).

Thus, in the present study, we aimed to examine whether the inotropic effects of

nifekalant are altered in MCT-induced heart failure in rats, and if so, to examine the

mechanisms involved.

Methods

Animal Model

All animal procedures were performed according to the guidelines for the care and use of laboratory animals of Tohoku University. A total of 92 Sprague-Dawley rats weighing 200 g were used. They received a single subcutaneous injection of 0.5 mL 60 mg/kg monocrotaline (Uzzaman et al., 2000) (MCT-rats) or an equal volume of solvent (Ctr-rats). Four weeks after the injection, 25.4 % of the MCT-rats died due to right-sided heart failure while no Ctr-rats died. The survivors were anesthetized and the right atrial and ventricular pressures were measured with a 2 F catheter inserted from the right jugular vein. Pressure signals were digitized at a rate of 0.5 kHz for 3 min. After the pressure measurement, the heart was excised for preparation of samples and measurement of heart weight.

Preparation of Samples

65 trabeculae were obtained from 65 rats as previously described (Miura et al., 1999; Wakayama et al., 2005). Trabeculae were dissected from the right ventricle and equilibrated at 0.5 Hz stimuli through parallel platinum electrodes in the bath with 5 ms pulses 50 % above the threshold ($[Ca^{2+}]_o = 0.7$ mM) at room temperature. Force was measured using a silicon semiconductor strain gauge and expressed as stress after normalizing for the cross sectional area of the muscle measured in the slack conditions. The sarcomere length was measured using laser diffraction techniques (ter Keurs et al., 1980; Wakayama et al., 2005). Membrane potential was measured using ultracompliant glass microelectrodes, as previously described (Hirose et al.,

2005). To estimate the duration of action potential, the time to 90 % repolarization of the action potential (APD_{90}) was measured.

Fura-2 Loading and Measurement of Fluorescence

$[Ca^{2+}]_i$ was measured as previously described (Miura et al., 1999; Wakayama et al., 2005). Briefly, fura-2 pentapotassium salt was microinjected electrophoretically into one cell and allowed to spread uniformly throughout the trabeculae via the gap junctions. The epifluorescence of fura-2 from the trabecula at excitation wavelengths of 340 and 380 nm was measured at 510 nm by a photomultiplier tube (E1341 with a C1556 socket, Hamamatsu, Japan). The signal from the photomultiplier tube was stored (RD-130TE DAT Data Recorder, TEAC, Japan) and used for the calculation of $[Ca^{2+}]_i$ after the subtraction of the autofluorescence. The decline of Ca^{2+} transients was expressed as the time constant of the decay calculated from the fit of a monoexponential function to the decline of Ca^{2+} transients.

Rapid Cooling Contracture (RCC)

SR Ca^{2+} content was estimated using a RCC technique as previously described (Hirose et al., 2005). The perfusion line filled with a warm solution (~24 ^{o}C) was instantly replaced by another perfusion line that was jacketed with ethylene glycol-water (1:3 at -5 ^{o}C) in response to a voltage command from a personal computer. This switching from the warm solution to the cold solution cooled the muscle surface to below 1 ^{o}C in less than 1 second and maintained steadily the bath temperature at ~1 ^{o}C during the perfusion of cold solution. The time courses of cooling were sufficiently rapid to produce reproducible RCCs.

Quantitative Immunoblotting Analysis of SR Ca^{2+} Cycling Proteins

The expression levels of sarcoplasmic reticulum ATPase type2 (SERCA2), phospholamban (PLB), ryanodine receptor type2 (RyR2), sodium-calcium exchanger (NCX), and glyceraldehyde-3-phosphate dehydrogenase (GAPDH) as an internal standard were measured as previously described (Takahashi et al., 2003). The tissue of the right ventricular free wall (10 μg for SERCA2; 10 μg for PLB; 150 μg for RyR2; 150 μg for NCX; 10 μg for GAPDH) was homogenized in 20 mM Tris aminomethane maleate containing 0.3 M sucrose, 0.1 M KCl, 5 mg/L leupeptin, and 0.1 mM phenylmethylsulfonyl fluoride, at pH 7.0. Cardiac homogenates were separated on SDS-PAGE, in which a proper percentage of acrylamide was selected according to the targeted protein (7.5 % for SERCA2; 12 % for PLB; 3-12 % gradient gel for RyR and NCX; 10 % for GAPDH), and electrophoresis was run at 150 V for 1 hour. Proteins were then transferred to nitrocellulose membranes and the membranes were reacted with mouse monoclonal antibodies against SERCA2, PLB, RyR2, NCX, and GAPDH (Affinity Bioreagents, Golden, CO) at a dilution of 1:1000. After washing, the blots were incubated with a peroxidase-conjugated secondary antibody (Sigma, Saint Louis, MO) at a dilution of 1:1000. The protein bands were visualized using an enhanced chemiluminescence (ECL) detection system (Amersham, Arlington, IL) and the optical density was quantified using Image Gauge after scanning with Image Reader LAS-1000 (Fuji Film, Tokyo, Japan). The expression level of each protein was normalized to that of GAPDH. We have verified the linearity of the ECL detection system by measuring the expression levels of

GAPDH in different amounts of tissue (5, 10, 15, and 20 µg) from the right ventricular

free wall.

Experimental Protocol

We examined the effects of nifekalant on action potentials, Ca^{2+} transients and

developed forces in 7 trabeculae and on RCCs in 5 trabeculae. Trabeculae were

stimulated electrically at 0.5 or 2.0 Hz and superfused with HEPES solution

containing nifekalant ($[Ca^{2+}]_o$ = 0.7 mM, temperature = 26.0 ± 0.2 ^{o}C, sarcomere

length (SL) = 2.1 µm). At first, we used 1 and 10 µM nifekalant, because the

therapeutic concentration of the agent ranges from 1 to 10 µM (Shiga et al., 2001),

and then we used 250 µM nifekalant to examine its effect on cardiac muscle at an

extremely high concentration (250 µM) (Mori et al., 1995). All measurements were

completed within 20 min. To inhibit the SR function, we exposed the trabeculae to 30

µM cyclopiazonic acid (CPA) and 1 µM ryanodine (Kentish and Wrzosek, 1998). Six

hours after the exposure to CPA and ryanodine, the remaining developed force was

measured at 0.5 Hz stimulation in 5 trabeculae from each group ($[Ca^{2+}]_o$ = 2.0 mM,

temperature = 26.0 ± 0.2 ^{o}C, SL = 2.1 µm).

Statistics

All measurements were expressed as mean ± SEM. Statistical analysis was

performed using ANOVA and paired Student t tests as appropriate. Values of P <

0.05 were considered to be statistically significant.

Results

Properties of MCT-Rats

The physiological profiles of Ctr-rats and MCT-rats are summarized in Table 1. Right ventricular pressure was higher and wet tissue weight of the right ventricular free wall was heavier in MCT-rats, suggesting that right ventricular hypertrophy was induced by the pulmonary hypertension. The contractile properties of Ctr-rats and MCT-rats are shown in Fig.1 and Table 2. The time to 90 % repolarization of the action potential was longer in MCT-rats. In MCT-rats, the amplitude of the developed force was reduced with a longer time-to-peak force, the Ca^{2+} transients declined more slowly after reaching the reduced peak values, and the amplitude of the RCCs, which may reflect the SR Ca^{2+} content, was lower.

To investigate the alteration in the adenylyl cyclase signaling pathway in MCT-rats, we examined the effect of forskolin on the developed force (Fig. 2A). Forskolin (1 μM) increased the developed force more than two times in Ctr-rats, but not in MCT-rats. The force-frequency relationship was also markedly different between the two groups; it was positive in Ctr-rats, but negative in MCT-rats (Fig. 2B). To determine the relative contribution of the Ca^{2+} entering through the sarcolemma to muscle contraction, SR function was inhibited with 30 μM CPA and 1 μM ryanodine. This SR inhibition reduced the developed force more in Ctr-rats than in MCT-rats (Fig. 2C), showing that the Ca^{2+} transport through the sarcolemma plays a more important role in the muscle contraction in MCT-rats compared with Ctr-rats.

Concerning the expression of Ca^{2+} handling proteins (Fig. 3), SERCA2 and the SERCA2/PLB ratio were significantly lower in MCT-rats, consistent with the slower

decline of the Ca^{2+} transients and the reduced amplitude of RCCs. The other Ca^{2+} handling proteins were almost identical for Ctr- and MCT-rats (Fig. 3).

Effect of Nifekalant

Nifekalant prolonged the duration of action potential equally in Ctr- and MCT-rats in a concentration-dependent manner (Fig. 4A). Nifekalant increased the developed force and the peak value of Ca^{2+} transient in Ctr-rats, but, surprisingly, nifekalant could not increase, but rather decreased them in MCT-rats at both 0.5 and 2.0 Hz stimulation (Figs. 4B, 4C). In MCT-rats nifekalant had no effect on the decline of Ca^{2+} transients, which may largely reflect the function of SR Ca^{2+} uptake, while in Ctr-rats the Ca^{2+} transients declined faster with nifekalant (Fig. 4D). Because Ca^{2+} for contraction originates from both the SR and the extracellular medium in mammalian cardiac muscle, we first examined the contribution of the SR Ca^{2+} using the RCCs technique. As shown in Figs. 5A and 5B, nifekalant increased the amplitude of RCCs in Ctr-rats, but not in MCT-rats, showing that nifekalant cannot increase the SR Ca^{2+} content in MCT-rats. We then examined the contribution Ca^{2+} entering through the sarcolemma with CPA and ryanodine. With the SR inhibited, nifekalant increased the force in Ctr-rats, but not in MCT-rats (Fig. 5C), showing that nifekalant cannot increase the Ca^{2+} entry through the sarcolemma in MCT-rats.

Discussion

The novel finding of the present study was that the positive inotropic effects of nifekalant were reduced in failing heart in rats, partly due to the reduced reserve of the trans-sarcolemmal Ca^{2+} transport and the depressed SR Ca^{2+} uptake. To the best of our knowledge, this is the first study that demonstrates the reduced positive inotropic effects of a class III anti-arrhythmic agent that is widely used in the treatment of arrhythmia in patients with heart failure for its positive inotropic effects noted in normal hearts.

Properties of MCT-Rats

It has been reported that isolated myocytes obtained from dysfunctional myocardium contract normally under basal (Anand et al., 1997; Prahash et al., 2000) and stimulated conditions (Prahash et al., 2000), whereas left ventricular contractile dysfunction due to tachycardia-induced cardiomyopathy can be improved without normalization of the myocyte function (Spinale et al., 1995). These discrepancies may be due to differences in the hemodynamic load, chamber geometry, and cell-cell or cell matrix connectivity between these preparations. Therefore, to fill the gap between isolated myocytes and whole hearts (Houser SR and Margulies, 2003), we used in this study multicellular ventricular muscle with the original cell-cell and cell-matrix connectivity (Sys et al., 1998), and measured the contractile properties with the proper load at the sarcomere length of 2.1 μm (Miura et al., 1999; Hirose et al., 2005).

It has been reported that pulmonary hypertension causes right ventricular hypertrophy with several alterations in a monocrotaline-treated model of rats (Kögler et al., 2003; Leineweber et al., 2003; Uzzaman et al., 2003). In agreement with the previous findings, the right ventricle of MCT-rats in this study showed ventricular hypertrophy due to pulmonary hypertension (Table 1), a longer action potential duration (Table 2, Fig. 1A), blunted response to forskolin (Fig. 2A), decreased protein expression of SERCA2 (Fig. 3), and a negative force-frequency relationship (Fig. 2B). Additionally, we were able to demonstrate for the first time in this model the decreased ratio in the protein expression of SERCA2 to PLB (Fig. 3) with a slower decline of Ca^{2+} transients and diminished SR Ca^{2+} content (Table 2), causing diminished contraction, especially at a higher stimulation frequency (Fig. 2B) (Ji et al., 2000; Periasamy and Huke, 2001). Moreover, SR inhibition reduced the developed force more in Ctr-rats than in MCT-rats (Fig. 2C), showing that the Ca^{2+} transporting function through the sarcolemma was relatively activated in MCT-rats. This greater fractional contribution of Ca^{2+} transport through the sarcolemma results in a reduction of the SR Ca^{2+} content (Piacentino et al., 2003). These findings described above have also been reported in mammalian left ventricular failing hearts, (Näbauer and Kääb, 1998; Hasenfuss and Pieske, 2002) including that of humans (Rossman et al., 2004; Meyer et al., 1995), suggesting that this MCT-treated model of rats can serve as a model of failing hearts to examine the electrophysiological alterations of the ventricle.

Effects of Nifekalant

Rat ventricular muscle possesses the I_{kr} (Pond et al., 2000). Nifekalant inhibits the I_{Kr} at therapeutic concentrations between 1 and 10 μM (Shiga et al., 2001) and inhibits

several other channels at concentrations above 10 μmol/L (Mori et al., 1995). Thus, it

is likely that the prolongation of action potential at 1 and 10 μ M nifekalant resulted

from the blocking action of I_{Kr} and that the further prolongation of action potential at

250 μM nifekalant resulted from the decrease in the outward currents due to the

blocking of other K channels (Fig. 4A). In agreement with our previous report (Hirose

et al., 2005), the prolongation of action potential in Ctr-rats increased Ca^{2+} entry

through the sarcolemma (Fig. 5C) (Stemmer and Akera, 1986), hastened SR Ca^{2+}

uptake probably due to the higher peak of Ca^{2+} transients (Fig. 4D) (Bers and Berlin,

1995), increased SR Ca^{2+} content (Fig. 5B), and ultimately induced more Ca^{2+}

release from the SR to activate more fully the myofilaments (Figs. 4B, 4C) (Shannon

et al., 2000). In contrast, in MCT-rats, the further prolongation of action potential by

nifekalant could not increase Ca^{2+} entry through the sarcolemma (Fig. 5C) or SR

Ca^{2+} loading in MCT-rats (Fig. 5B), resulting in no increase in the developed force

(Fig. 4B). NCX function, SERCA function, and diastolic SR Ca^{2+} leak may all be

involved in the differences between Ctr- and MCT-treated rats, because these three

factors can contribute to SR Ca^{2+} loading (Shannon et al., 2003).

First of all, the impairment of SR Ca^{2+} uptake may be largely responsible for the

differences between Ctr- and MCT-rats, because in MCT-rats nifekalant had no

effect on SR Ca^{2+} uptake (Fig. 4D) and consequently had no effect on SR Ca^{2+}

content (Fig. 5B). Additionally, the MCT-rats showed a negative force-frequency

relationship (Fig. 2B), suggesting that the reserve of SR Ca^{2+} uptake was diminished

in those rats (Pieske et al., 1999). This impairment of SR Ca^{2+} uptake may reduce

the inotropic effect of nifekalant in MCT-rats (Fig. 4B). Second, the alteration in the

Ca^{2+} transport through the sarcolemma may also concern the differences. This is

probably because the Ca^{2+} transporting function through the sarcolemma was fully activated in MCT-rats with the prolongation of action potential (Chen et al., 2002, Wei et al., 2003). Under this condition, further prolongation of the action potential induced by nifekalant could have only a limited effect on the integrated Ca^{2+} influx (Fig. 5C), because too many Ca^{2+} channels had already been unresponsive (Yuan et al., 1996). This alteration in the Ca^{2+} transport through the sarcolemma can directly alter the Ca^{2+} supply to myofilaments or indirectly alter it by changing the SR Ca^{2+} loading (Ranu et al., 2002). Finally, leak of the SR Ca^{2+} may contribute minimally to the alteration in SR Ca^{2+} content in MCT-rats (Shannon et al., 2003), because SR inhibition could not restore the developed force in those rats.

Clinical Implications

Because ventricular arrhythmias often occur in patients with reduced left ventricular ejection fractions, it is important for physicians to understand the inotropic effects of anti-arrhythmic agents, especially in failing hearts. D-sotalol, which has class III anti-arrhythmic activity, exerts a positive inotropic effect in the intact canine heart (Peralta et al., 2000), whereas it has no positive inotropic effect in failing and non-failing human left ventricular myocardium, probably due to the contamination of L-sotalol with ß-adrenoceptor-blocking properties (Holubarsch et al., 1995). In this study, nifekalant exerted positive inotropic effects in Ctr-rats whereas no such effect was noted in MCT-rats, indicating that the inotropic effects of nifekalant are markedly reduced in failing hearts, although nifekalant still has an anti-arrhythmic effect in failing hearts (Katoh et al., 2005). Thus, it should be noted that the inotropic effects of class III anti-arrhythmic agents could be reduced or even absent in patients with heart failure.

References

Anand IS, Liu D, Chugh SS, Prahash AJC, Gupta S, John R, Popescu F, Chandrashekhar Y (1997) Isolated myocyte contractile function is normal in postinfarct remodeled rat heart with systolic dysfunction. *Circulation* 96:3974-3984.

Bers DM, Berlin JR (1995) Kinetics of [Ca]$_i$ decline in cardiac myocytes depend on peak [Ca]$_i$. *Am J Physiol* 268:C271-C277

Chen X, Piacentino V III, Furukawa S, Goldman B, Margulies KB, Houser SR (2002) L-type Ca^{2+} channel density and regulation are altered in failing human ventricular myocytes and recover after support with mechanical assist devices. *Circ Res* 91:517-524.

Hasenfuss G, Pieske B (2002) Calcium cycling in congestive heart failure. *J Mol Cell Cardiol* 34:951-969.

Hirose M, Miura M, Wakayama Y, Endo H, Sugai Y, Stuyvers BDMY, Kagaya Y, Watanabe J, ter Keurs HEDJ, Shirato K (2005) Effect of nifekalant, a class III anti-arrhythmic agent, on Ca^{2+} waves in rat intact trabeculae. *Circ J* 69:739-745.

Holubarsch C, Schneider R, Pieske B, Ruf T, Hasenfuss G, Fraedrich G, Posival H, Just H (1995) Positive and negative inotropic effects of DL-sotalol and D-sotalol in failing and nonfailing human myocardium under physiological experimental conditions. *Circulation* 92:2904–2910.

Houser SR, Margulies KB (2003) Is depressed myocyte contractility centrally involved in heart failure? *Circ Res* 92:350-358.

Ji Y, Lalli MJ, Babu GJ, Xu Y, Kirkpatrick DL, Liu LH, Chiamvimonvat N, Walsh RA,
Shull GE, Periasamy M (2000) Disruption of a single copy of the SERCA2 gene
results in altered Ca^{2+} homeostasis and cardiomyocyte function. *J Biol Chem*
275:38073-38080.

Katoh T, Mitamura H, Matsuda N, Takano T, Ogawa S, Kasanuki H (2005)
Emergency treatment with nifekalant, a novel class III anti-arrhythmic agent, for
life-threatening refractory ventricular tachyarrhythmias. Post-marketing special
investigation. *Circ J* 69:1237-1243.

Kentish JC, Wrzosek A (1998) Changes in force and cytosolic Ca^{2+} concentration
after length changes in isolated rat ventricular trabeculae. *J Physiol* 506:431-
444.

Kögler H, Hartmann O, Leineweber K, Nguyen van P, Schott P, Brodde O-E,
Hasenfuss G (2003) Mechanical load-dependent regulation of gene expression
in monocrotaline-induced right ventricular hypertrophy in the rat. *Circ Res*
93:230-237.

Krishnan SC, Schuger CD, Goldstein S (2002) Sudden death in heart failure:
underlying electrophysiological mechanisms. *Heart Fail Rev* 7:255-260.

Leineweber K, Brandt K, Wludyka B, Beilfuss A, Pönicke K, Heinroth-Hoffmann I,
Brodde O-E (2002) Ventricular hypertrophy plus neurohumoral activation is
necessary to alter the cardiac ß-adrenoceptor system in experimental heart
failure. *Circ Res* 91:1056-1062.

Meyer M, Schillinger W, Pieske B, Holubarsch C, Heilmann C, Posival H, Kuwajima
G, Mikoshiba K, Just H, Hasenfuss G (1995) Alterations of sarcoplasmic
reticulum proteins in failing human dilated cardiomyopathy. *Circulation* 92:778-
784.

Miura M, Boyden PA, ter Keurs HEDJ (1999) Ca^{2+} waves during triggered propagated contractions in intact trabeculae. Determinants of the velocity of propagation. *Circ Res* 84:1459-1468.

Mori K, Hara Y, Saito T, Masuda Y, Nakaya H (1995) Anticholinergic effects of class III antiarrhythmic drugs in guinea pig atrial cells. Different molecular mechanisms. *Circulation* 91:2834-2843.

Näbauer M, Kääb S (1998) Potassium channel down-regulation in heart failure. *Cardiovasc Res* 37:324-334.

Nakaya H, Tohse N, Takeda Y, Kanno M (1993) Effects of MS-551, a new class III antiarrhythmic drug, on action potential and membrane currents in rabbit ventricular myocytes. *Br J Pharmacol* 109:157-163.

Peralta AO, John RM, Gaasch WH, Taggart PI, Martin DT, Venditti FJ (2000) The class III antiarrhythmic effect of sotalol exerts a reverse use-dependent positive inotropic effect in the intact canine heart. *J Am Coll Cardiol* 36:1404-1410.

Periasamy M, Huke S (2001) SERCA pump level is a critical determinant of Ca^{2+} homeostasis and cardiac contractility. *J Mol Cell Cardiol* 33:1053-1063.

Piacentino V III, Weber CR, Chen X, Weisser-Thomas J, Margulies KB, Bers DM, Houser SR (2003) Cellular basis of abnormal calcium transients of failing human ventricular myocytes. *Circ Res* 92:651-658.

Pieske B, Maier LS, Bers DM, Hasenfuss G (1999) Ca^{2+} handling and sarcoplasmic reticulum Ca^{2+} content in isolated failing and nonfailing human myocardium. *Circ Res* 85:38-46.

Pond AL, Scheve BK, Benedict AT, Petrecca K, van Wagoner DR, Shrier A, Nerbonne JM (2000) Expression of distinct ERG proteins in rat, mouse, and human heart. Relation to functional I_{Kr} channels. *J Biol Chem* 275:5997-6006.

Prahash AJC, Gupta S, Anand IS (2000) Myocyte response to ß-adrenergic stimulation is preserved in the noninfarcted myocardium of globally dysfunctional rat hearts after myocardial infarction. *Circulation* 102:1840-1846.

Ranu HK, Terracciano CMN, Davia K, Bernobich E, Chaudhri B, Robinson SE, Kang ZB, Hajjar RJ, MacLeod KT, Harding SE (2002) Effects of Na^+/Ca^{2+}-exchanger overexpression on excitation-contraction coupling in adult rabbit ventricular myocytes. *J Mol Cell Cardiol* 34:389-400.

Rossman EI, Petre RE, Chaudhary KW, Piacentino V 3rd, Janssen PML, Gaughan JP, Houser SR, Margulies KB (2004) Abnormal frequency-dependent responses represent the pathophysiologic signature of contractile failure in human myocardium. *J Mol Cell Cardiol* 36:33-42.

Seyfarth T, Gerbershagen H-P, Giessler C, Leineweber K, Heinroth-Hoffmann I, Pönicke K, Brodde O-E (2000) The cardiac ß-adrenoceptor-G-protein(s)-adenylyl cyclase system in monocrotaline-treated rats. *J Mol Cell Cardiol* 32:2315-2326.

Sen L, Cui G, Sakaguchi Y, Singh BN (1998) Electrophysiological effects of MS-551, a new class III agent: comparison with dl-sotalol in dogs. *J Pharmacol Exp Ther* 285:687-694.

Shannon TR, Ginsburg KS, Bers DM (2000) Potentiation of fractional sarcoplasmic reticulum calcium release by total and free intra-sarcoplasmic reticulum calcium concentration. *Biophys J* 78:334-343.

Shannon TR, Pogwizd SM, Bers DM (2003) Elevated sarcoplasmic reticulum Ca^{2+} leak in intact ventricular myocytes from rabbits in heart failure. *Circ Res* 93:592–594.

Shiga T, Ando S, Suzuki T, Matsuda N, Kasanuki H (2001) Reverse use-dependent QT prolongation during infusion of nifekalant in a case of recurrent ventricular tachycardia with old myocardial infarction. *J Electrocardiol* 34:77-80.

Spinale FG, Holzgrefe HH, Mukherjee R, Arthur SR, Child MJ, Powell JR, Koster WH (1995) LV and myocyte structure and function after early recovery from tachycardia-induced cardiomyopathy. *Am J Physiol* 268:H836-H847.

Stemmer P, Akera T (1986) Concealed positive force-frequency relationships in rat and mouse cardiac muscle revealed by ryanodine. *Am J Physiol* 251:H1106-H1110.

Sys SU, De Keulenaer GW, Brutsaert DL (1998) Reappraisal of the multicellular preparation for the in vitro physiopharmacological evaluation of myocardial performance. *Adv Exp Med Biol* 453:441-450.

Takahashi J, Kagaya Y, Kato I, Ohta J, Isoyama S, Miura M, Sugai Y, Hirose M, Wakayama Y, Ninomiya M, Watanabe J, Takasawa S, Okamoto H, Shirato K (2003) Deficit of CD38/cyclic ADP-ribose is differentially compensated in hearts by gender. *Biochem Biophys Res Commun* 312:434-440.

ter Keurs HEDJ, Rijnsburger WH, van Heuningen R, Nagelsmit MJ (1980) Tension development and sarcomere length in rat cardiac trabeculae. Evidence of length -dependent activation. *Circ Res* 46:703-14.

Uzzaman M, Honjo H, Takagishi Y, Emdad L, Magee AI, Severs NJ, Kodama I (2000) Remodeling of gap junctional coupling in hypertrophied right ventricles of rats with monocrotaline-induced pulmonary hypertension. *Circ Res* 86:871-878.

Wakayama Y, Miura M, Stuyvers BD, Boyden PA, ter Keurs HEDJ (2005) Spatial nonuniformity of excitation-contraction coupling causes arrhythmogenic Ca^{2+} waves in rat cardiac muscle. *Circ Res* 96:1266-73.

Wei S-K, Ruknudin A, Hanlon SU, McCurley JM, Schulze DH, Haigney MCP (2003)

Protein kinase A hyperphosphorylation increases basal current but decreases ß-

adrenergic responsiveness of the sarcolemmal Na^+-Ca^{2+} exchanger in failing pig

myocytes. *Circ Res* 92:897-903.

Yuan W, Ginsburg KS, Bers DM (1996) Comparison of sarcolemmal calcium

channel current in rabbit and rat ventricular myocytes. *J Physiol* 493.3:733-746.

Footnotes

Legends for Figures

Figure 1.

Representative recordings of action potential (A), developed force (B), and Ca^{2+} transient (C) in Ctr-rats (thick line) and MCT-rats (thin line) at 0.5 Hz stimulation.

Figure 2.

Effects of forskolin, the stimulation frequency, and the SR inhibition on the developed force. Results are expressed as mean $\pm$ SEM. * P< 0.05 vs Ctr-rats (control).

Panel A: Upper panel shows representative recordings in the absence (thin line) and the presence of 1 μM forskolin (thick line) at 0.5 Hz stimulation and the lower panel shows the summed data obtained from 5 trabeculae. In the upper panel, 1 μM forskolin increased the developed force almost two times in Ctr-rats (left panel, Control), but not in MCT-rats (right panel, MCT). In the lower panel, the increase in the developed force by 1 μM forskolin was significantly higher in Ctr-rats than that in MCT-rats.

Panel B: Force-frequency relationship in Ctr-rats (n = 4) and MCT-rats (n = 4). Ctr-rats (open circle) showed the positive force-frequency relationship, while MCT-rats (closed circle) showed the negative one.

Panel C: Effect of SR inhibition on the developed force in Ctr-rats (n =5, open circle) and MCT-rats (n = 5, closed circle). SR inhibition with 30 µM cyclopiazonic acid and 1µM ryanodine reduced the developed force to 9.8 ± 2.5 % in Ctr-rats and to 28.5 ± 2.5 % in MCT-rats. The remaining ratio of the developed force after the SR inhibition was significantly larger in MCT-rats.

Figure 3.

Expression levels of Ca^{2+} handling proteins in Ctr-rats (n = 5) and MCT-rats (n = 5).

Panel A: Examples of Western blots.

Panel B: Expression levels of Ca^{2+} handling proteins after normalization to the protein level of GAPDH. SR ATPase type2 (SERCA2) and the SERCA2/phospholamban (PLB) ratio were lower in MCT-rats. The protein expression of PLB, ryanodine receptor (RyR), and sodium-calcium exchanger (NCX) was comparable between the two groups. Results are expressed as mean ± SEM. * P< 0.05 vs Ctr-rats (control).

Figure 4.

Effects of nifekalant on action potential, the developed force, and Ca^{2+} transients. Results are expressed as mean ± SEM. * P< 0.05 vs. Ctr-rats (control), † P < 0.05 vs. no nifekalant.

Panel A: Effect of nifekalant on the duration of action potential at 90 % repolarization (APD_{90}) obtained from Ctr-rats (open circle, n=4) and MCT-rats (closed circle, n=3). Nifekalant increased the APD_{90} equally in the two groups.

Panel B: Effect of nifekalant on the force obtained from trabeculae of Ctr-rats (0.5 Hz stimulation; open circle, 2 Hz stimulation; open square, n=5) and those of MCT-rats (0.5 Hz stimulation; closed circle, 2 Hz stimulation; closed square, n=9). At both stimulation frequencies, nifekalant increased the force in Ctr-rats but not in MCT-rats.

Panel C: Effect of nifekalant on the peak Ca^{2+} transient obtained from trabeculae of Ctr-rats (0.5 Hz stimulation; open circle, 2 Hz stimulation; open square, n=4) and those of MCT-rats (0.5 Hz stimulation; closed circle, 2 Hz stimulation; closed square, n=7). At both stimulation frequencies, nifekalant increased the Ca^{2+} transient in Ctr-rats but not in MCT-rats.

Panel D: Effect of nifekalant on the decline of Ca^{2+} transient at 0.5 Hz stimulation obtained from trabeculae of Ctr-rats (open circle, n=4) and those of MCT-rats (closed circle, n=7). Nifekalant had no effect on the decline of Ca^{2+} transients in MCT-rats, while in Ctr-rats Ca^{2+} transients declined faster with nifekalant (left panel). Ca^{2+} transients declined more slowly in MCT-rats at all over the concentrations of nifekalant tested (right panel).

Figure 5.

Effect of nifekalant on contractures induced by rapid-cooling (RCCs) and the force under the condition of SR inhibition. Results are expressed as mean $\pm$ SEM. * P< 0.05 vs. Ctr-rats (control), † P < 0.05 vs no nifekalant.

Panel A: Representative tracings of RCCs in the absence (thin line) and presence of 250µM nifekalant (thick line). Trabeculae were stimulated electrically at 0.5 Hz until the twitch force reached complete equilibration. Two seconds after the last electrical stimulus, rapid switching from a warm solution to a cold solution induced RCCs ($[Ca^{2+}]_o$ = 0.7 mM). Nifekalant increased the amplitude of the RCC in Ctr-rats (left panel) but not in MCT-rats (right panel). s: electrical stimulation.

Panel B: Effect of nifekalant on the RCCs obtained from trabeculae of Ctr-rats (open circle, n=5) and those of Mct-rats (closed circle, n=5). Nifekalant increased the amplitude of RCCs in Ctr-rats but not in MCT-rats.

Panel C: Effect of nifekalant on the force obtained from trabeculae of Ctr-rats (open circle, n=5) and those of MCT-rats (closed circle, n=5) with the SR inhibited with CPA and ryanodine. Under this condition, nifekalant increased the force in Ctr-rats but not in MCT-rats.

Tables

Table 1. Physiological profiles of animals

	Control	MCT
BW (g)	346±13	306±11*
HR (bpm)	356±10	328±15
RVP (mmHg)	20.6±0.9	51.4±2.0*
RV/body wt (mg/g)	0.59±0.05	1.33±0.04*
(LV+Septum)/ body wt (mg/g)	2.11±0.08	2.23±0.06
RV/(LV+Septum)	0.28±0.02	0.60±0.03*

Control, control rats (n =18); MCT, monocrotaline-treated rats (n=20); BW, body

weight; HR, heart rate; RVP, right ventricular pressure; RV, right ventricle; wt,

weight; LV, left ventricle; RV/LV+Septum, a ratio of RV weight to LV weight.

Results are expressed as mean $\pm$ SEM.   *P<0.05 vs. control rats.

Table 2. Membrane potential, developed force, and Ca^{2+} transient

Pacing frequency	0.5Hz		2.0 Hz	
	Control	MCT	Control	MCT
APD_{90} (ms)	184 ± 19	314 ± 36*		
Force (mN/mm^2)	28 ± 5	19 ± 2*	33 ± 6	16 ± 2*
TTP Force (ms)	169 ± 21	237 ± 9*	138 ± 16	184 ± 11*
Peak $[Ca^{2+}]_i$ (nM)	955 ± 70	900 ± 22	1038± 58	886 ± 16*
$[Ca^{2+}]_i$ decline (ms)	161 ± 26	271 ±33*	120 ± 25	167 ± 18*
Diastolic $[Ca^{2+}]_i$ (nM)	87 ± 11	100 ± 23	112 ± 13	173 ± 25
RCC Amplitude (mN/mm^2)	45 ± 6	31 ± 2*		

Control, control rats (n =5); MCT, monocrotaline-treated rats (n=5-7); TTP, time to peak activation of force; RCC, Rapid Cooling Contracture. Results are expressed as mean ± SEM. *P<0.05 vs. control rats.
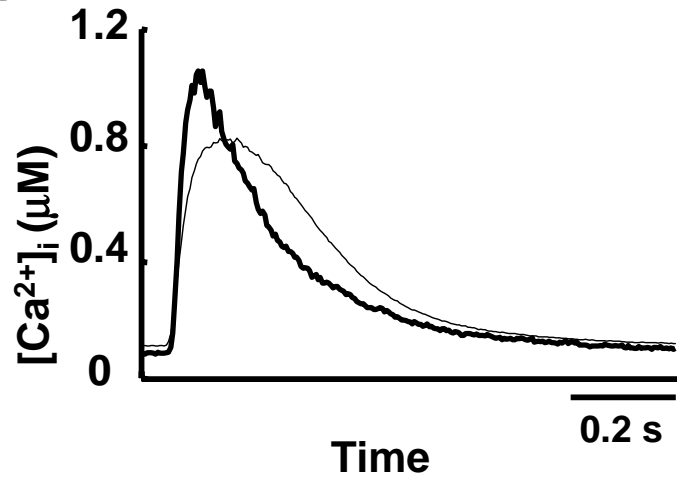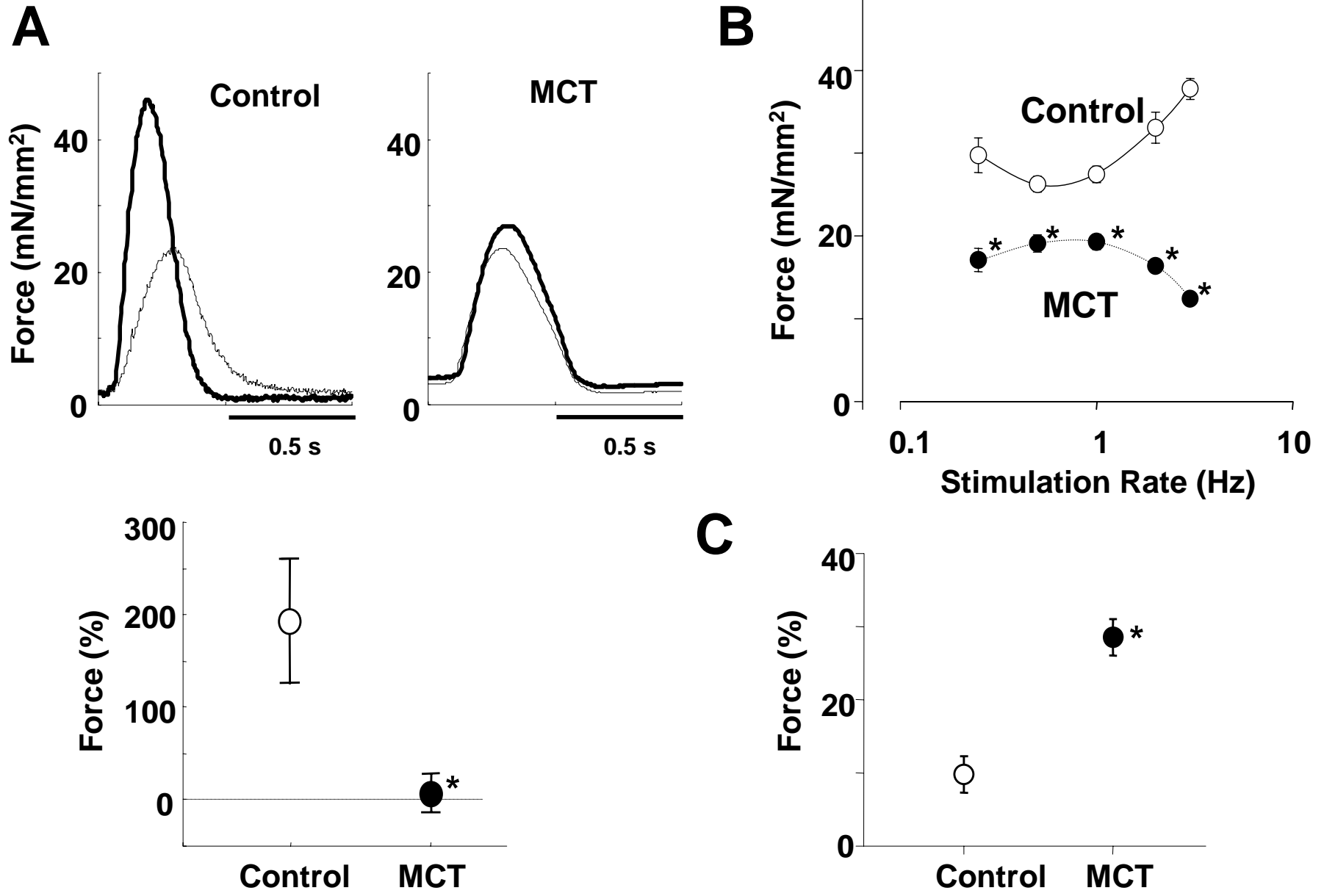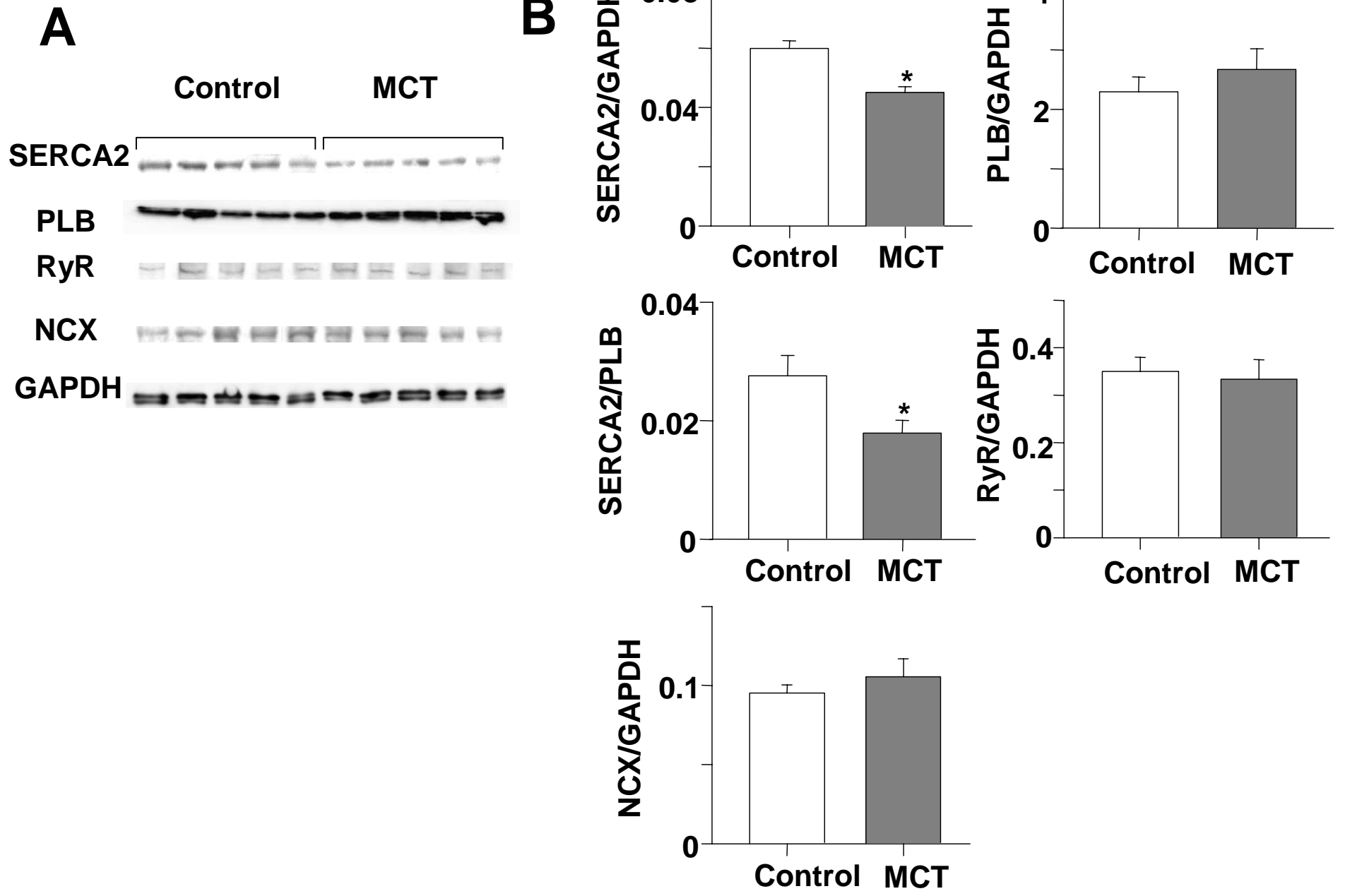
Figure.1

Figure.2

Figure. 3

A

B

Figure.4

Figure.5